

QSAR Studies of Flavonoids and Isoflavonoids with PTP1B: A Potential Pharmacological Target for the Treatment of Insulin Resistance

PRANGYA RATH¹, ANUJ RANJAN^{2,*}, ABHISHEK CHAUHAN^{2,*}, NAVAL KUMAR VERMA³ and TANU JINDAL²

¹Amity Institute of Environmental Sciences, Amity University Uttar Pradesh, Noida-201303, India

²Amity Institute of Environmental Toxicology Safety and Management, Amity University Uttar Pradesh, Noida-201303, India

³Ministry of Ayush, Ayush Bhawan, B Block, GPO Complex INA New Delhi-110023, India

*Corresponding author: E-mail: aranjan@amity.edu; akchauhan@amity.edu

Received: 24 January 2022;

Accepted: 28 February 2022;

Published online: 10 March 2022;

AJC-20750

This study deals with designing and validating QSAR models generated for 45 flavonoids having PTP1B inhibition properties. Eight molecular descriptors/pharmacophoric features of each flavonoid along with their reported IC₅₀ values against PTP1B were utilized to prepare training sets and generate models. It was developed by employing linear regression to calculate the predicted IC₅₀ values. The generated models were validated using reported IC₅₀ values of test sets. The correlation R² values were observed to be in the following order, 92.45% (for an increasing hydrogen bond donor), 92.08% (for randomly sorting), 91.85% (for increasing molecular weight), 84.19% (for increasing hydrogen bond acceptor), 64.91% (for increasing TPSA), 53.90% (for increasing number of rotatable bonds) and 52.28% (for increasing log P); signifying the role of these pharmacophoric features while drug designing. Molecular docking of the flavonoids with the PTP1B active site revealed interactions with catalytic site and adjacent loops. The models would be beneficial for further studies for drug designing against PTP1B inhibition and therapeutic implications for treatment of insulin resistance.

Keywords: Insulin resistance, QSAR, Flavonoids, PTP1B, Inhibition, Treatment.

INTRODUCTION

Insulin resistance is a condition of impaired biologic response to insulin hormone by tissues; resulting in impaired glucose disposal, hyperglycemia, hyperuricemia, increased insulin production by β -cell/hyperinsulinemia, cardiovascular disease, increased oxidative stress, cell damage, *etc.* [1,2]. The consequence of prolonged insulin resistance leads to the development of Type-2 diabetes mellitus (T2DM) and its associated complications [3,4]. Such alarming health consequences have medical attention towards designing drugs for treatment and cure of insulin resistance.

One of the fundamental goals in drug design is to predict the efficiency and efficacy of binding of a given molecule to a target. The computational approach of drug designing has become a powerful methodology to screen large libraries of ligands/compounds carrying desired drug-like properties. The techniques are gaining increasing preference by academicians, pharmaceuticals and many organizations as they are time-saving,

cost-effective, require comparatively fewer resources and manpower. Such bioinformatics approaches are data-driven and make it convenient to screen a large library of compounds/ligands during the early stages of research by giving informative outputs in a little span of time. An effective computational method involved in *in silico* drug designing technology is quantitative structure-activity relationship (QSAR). The QSAR technique plays a crucial role as it relates the chemical structures/properties of ligands to their biological activity. This technique is considered as an efficient process in virtual screening of drug designing as it is considered a validation tool in building mathematical models, finding statistically significant correlation and regression properties (like pIC₅₀, pEC₅₀, K_i, values, *etc.*), toxicology properties, classification properties, predicting biological properties of novel compounds, *etc.* [5,6].

Protein tyrosine phosphatase 1B (PTP1B) is a cytosolic protein which is associated with the pathogenesis of insulin resistance [7]. Higher expression of PTP1B leads to T2DM, obesity, autoimmune diseases [8,9]. Inhibition of PTP1B has

been observed to restore insulin signalling, thereby ameliorating insulin resistance [10]. Development of PTP1B inhibitors has been a challenging task because of high polar nature of the active site [8]. Hence, studies are now focused on developing potent inhibitors which comprises of synthetic compounds, natural products and hybrid compounds [11].

Flavonoids are one of the largest and important class of phytochemicals with an estimation of nearly 10,000 members that have low-molecular weight and belong to polyphenols [12,13]. These are secondary metabolites that is found in the most angiospermic plant parts like bark, roots, stems, flowers and widely available in many dietary fruits, vegetables, grains, nuts, beverages, herbs, medicinal plants, *etc.* [14]. They have gained wide popularity because they possess miscellaneous biochemical, detoxifying agents and antioxidative properties which are beneficial and favourable to cells. These have shown positive effects in fighting many diseases including Alzheimer's, atherosclerosis, blood pressure, cancer, cardiovascular ailments, diabetes, oxidative stress, inflammations, mutagenesis and many metabolic syndromes [14-16]. They are found in glycosylated or esterified forms. According to the variation in their substitution patterns or derivatives, degree of unsaturation and oxidation of the C-ring, they are classified into several subgroups such as flavones, flavanones, flavonols, flavan-3-ols, flavanonols, flavanols/catechins, anthocyanins, anthocyanidins, chalcones, isoflavans, isoflavones, pterocarpans, *etc.* [14,17,18].

Flavonoids extracted from various plant sources have been observed to be effective against PTP-1B inhibition [19-21]. They possess significant hypoglycemic effects, low toxicity for cells and are non-competitive inhibitors of PTP-1B [22]. The structure-activity relationship (SAR) studies have shown that their inhibitory activities are due to the presence of prenylated flavonoids and the prenyl group present on ring B. It has also been observed that the presence of less polar substituents (such as an isoprenyl group), or conversion of hydroxy group on the structures into less polar functionalities (by methylation or acetylation) usually enhanced the PTP-1B inhibitory activity; however the addition of hydroxyl group was seen to decrease the inhibitory activity [23]. A study conducted has revealed that the nature, position and number of substituents present in the flavonoid structure increased its ability to inhibit PTP1B. These substituents included the presence of both 7- and 8-OMe groups at C-7 and C-8 in ring A, together with the presence of both 3'- and 4'-OBn groups in B ring, which significantly improved PTP-1B inhibition. While lack of a double bond between C2=C3, addition of a hydroxyl group to C-5 in ring A, presence of a polar functionality (*e.g.* hydroxyl group) in ring B may be responsible for weakening the activity [24,25]. However, presence of an isoprenyl or methoxyl group at C-3' of ring B exhibited significant inhibitory activity [23]. Presence of another 4'-OH group in ring B slightly favoured PTP-1B inhibition [24]. Similarly the PTP-1B inhibitory activity of isoflavonoids was observed to be exhibited due to the presence of an isoprenyl group in the ring B and an *ortho*-hydroxyl group, for example presence of 2',4'-dihydroxy group in ring B of isoflavanoids correlated with its inhibitory activity [23,26].

Flavonoids improved insulin resistance by stimulating increasing insulin sensitivity, AMPK pathway, phosphorylation of insulin receptors and insulin receptor substrates and significantly enhancing glucose-uptake activity [22,23]. *In silico* studies of flavonoids have shown them to be potent allosteric inhibitors of PTP1B that bring about conformational changes and inactivate the protein [27]. Therefore, they are considered for their therapeutic implications.

A number of SAR studies have been observed for flavonoids and PTP1B [21,24], however, QSAR studies of flavonoids and PTP1B inhibition have not been reported much. QSAR is *in silico* approaches that formulate simple mathematical relationships between the biological activity of drug and physiological chemical properties [28-33]. It highlights that different structural properties of a compound contributes in a linear additive manner to showcase its biological activity. Therefore, such studies play a pivotal role in drug designing. This study aims for the creation, validation and accurate estimation of QSAR models for the prediction of the inhibition of flavonoids against PTP1B. As preliminary step of QSAR model development, the basic structure of compounds/flavonoids was kept similar. Relevant chemogenomics data, containing IC₅₀ values, were collected from the literature databases. Chemical descriptors highlighting different levels of representation of molecular structure/parameters were retrieved from ChemDes and then correlated with the biological property using machine learning techniques. Twenty eight QSAR models (training set and test set) with descriptors and regression coefficients were created by using EasyQSAR software and average R² was calculated. The models were used for prediction of PTP1B inhibition by flavonoids from the test set. The ligands were further subjected to docking for studying their binding energies with PTP1B active site and top hits were analyzed with their molecular descriptors.

EXPERIMENTAL

Preparation of database: A list of 45 flavonoids group (a class of polyphenols) with PTP-1B inhibitory activity (IC₅₀) was retrieved from literature reviews. The Canonical SMILES of the respective flavonoid was retrieved from NCBI-PubChem. Molecular descriptors of the flavonoid were derived using ChemDes website (<https://www.scbdd.com/chemdes>). Pharmacophore feature like molecular weight, H-bond acceptor (HBA/naccr), H-bond donor (HBD/ndonr), no: of rotatable bonds (nrot), number of aromatic bonds (naro), topological polar surface area (TPSA), logarithm of the molecules partition coefficient (log P) values, IC₅₀ and log IC₅₀ were tabulated for the study as depicted in Table-1.

Preparation of training set and test set: A series of rigorous sorting was done to prepare an unbiased training set and test set as shown in Table-2. Seven parameters were included in study and each parameter was sorted and divided into 4 set of ratios (50:50, 70:30, 75:25 and 25:75 ratio). As a result, a total of 28 methods were formulated. The parameters that were considered for model preparation were as follows: (1) Random sorting; (2) Increasing molecular weight; (3) Increasing HBA/naccr; (4) Increasing HBD/ndonr; (5) Increasing number of

TABLE-1
LIST OF 45 FLAVONOIDS WITH EXPERIMENTALLY REPORTED IC₅₀ VALUES AND MOLECULAR DESCRIPTORS

S. No.	Compound name	IC ₅₀ (μM)	log IC ₅₀	m.w.	HBA (naccr)	HBD (ndonr)	No. of rotatable bonds (nrot)	No. of aromatic bonds (naro)	TPSA	log P
1	Viscosol	13.5	1.13	388.24	7	2	6	17	98.36	4.40
2	Penduletin	57.9	1.76	328.19	7	2	4	17	98.36	2.89
3	5,6-Dihydroxy-3,4',7-trimethoxyflavone	32.2	1.50	328.19	7	2	4	17	98.36	2.89
4	Kaempferol 3-O-rutinoside	20.5	1.31	564.28	15	9	6	17	249.2	-1.39
5	Isorhamnetin-3-O-robinobioside	42.9	1.63	592.29	16	9	7	17	258.43	-1.38
6	Erybraedin A	2.4	0.38	364.27	4	2	4	12	58.92	5.72
7	Luteolin	6.70	0.82	276.15	6	4	1	17	111.13	2.28
8	2'-Methoxykurarinone	5.26	0.72	420.29	6	2	8	12	85.22	5.91
9	Mulberrofuran D	4.3	0.63	412.31	4	3	8	16	73.83	7.96
10	Mulberrofuran W	2.7	0.43	412.31	4	3	9	16	73.83	8.17
11	Catechin	2.24	0.35	276.15	6	5	1	12	110.38	1.54
12	Epicatechin	0.83	-0.07	276.15	6	5	1	12	110.38	1.54
13	<i>trans</i> -Resveratrol	16.1	1.20	216.15	3	3	2	12	60.69	2.97
14	Apigenin	24.76	1.39	260.16	5	3	1	17	90.9	2.57
15	Isovitexin	17.76	1.24	412.22	10	7	3	17	181.05	0.09
16	Vitexin	7.62	0.88	412.22	10	7	3	17	181.05	0.09
17	Isoorientin	24.54	1.38	428.22	11	8	3	17	201.28	-0.20
18	Orientin	57.11	1.75	428.22	11	8	3	17	201.28	-0.20
19	Abyssinin II/5'-prenylhomoeriodictyol	40.5	1.60	348.22	6	3	4	12	96.22	4.02
20	Parvisoflavone B	42.6	1.62	336.21	6	3	1	17	100.13	3.76
21	Neorautenol	7.6	0.88	304.21	4	1	0	12	47.92	4.18
22	Erybreadin D	4.2	0.62	364.27	4	1	2	12	47.92	5.69
23	Erybreadin B	7.8	0.89	364.27	4	1	2	12	47.92	5.69
24	Folitenol	6.4	0.80	364.27	4	1	2	12	47.92	5.69
25	Erysubin E	8.8	0.94	380.27	5	2	2	12	68.15	4.79
26	Erybreadin C	7.3	0.86	364.27	4	2	4	12	58.92	5.72
27	Licoagrone	6.0	0.77	700.48	10	5	10	24	170.82	8.71
28	Erythraddison III	4.6	0.66	332.22	5	2	4	12	75.99	3.97
29	Erysubin F	7.8	0.89	364.27	4	2	5	17	70.67	5.88
30	2'-Methoxykurarinone	5.26	0.72	420.29	6	2	8	12	85.22	5.91
31	Mimulone/bonannione A	1.9	0.27	380.27	5	3	6	12	86.99	5.74
32	3'-O-Methyl diplacone	3.9	0.59	408.28	6	3	7	12	96.22	5.75
33	6-Geranyl-3',5,5',7-tetrahydroxy-4'-methoxyflavanone	5.9	0.77	424.27	7	4	7	12	116.45	5.45
34	4'-O-Methyl diplacone	7.8	0.89	408.28	6	3	7	12	96.22	5.75
35	3'-O-Methyl diplacol	4.9	0.69	424.27	7	4	7	12	116.45	4.72
36	4'-O-Methyl diplacol	8.2	0.91	424.27	7	4	7	12	116.45	4.72
37	6-Geranyl-3,3',5,5',7-pentahydroxy-4'-methoxyflavane	6.6	0.81	424.27	7	5	7	12	119.61	4.79
38	Laxichalcone	20.7	1.31	380.27	5	2	3	12	75.99	5.36
39	Macarangin	22.7	1.35	396.26	6	4	6	17	111.13	5.51
40	Bonanniol A	15.2	1.18	396.26	6	4	6	12	107.22	4.71
41	7,4'-dimethylkaempferol/3,5-dihydroxy-7-methoxy-2-(4-methoxyphenyl)-4 <i>H</i> -chromen-4-one	16.92	1.22	300.18	6	2	3	17	89.13	2.88
42	(2 <i>S</i>)-5,6,7,3',4'-Pentamethoxyflavanone	6.88	0.83	352.21	7	0	6	12	72.45	3.43
43	3'-Hydroxy-3,5,7,4'-tetramethoxyflavone	22.25	1.34	340.20	7	1	5	17	87.36	3.2
44	3,5-Dihydroxy-7,3',4'-trimethoxyflavone	52.64	1.72	328.19	7	2	4	17	98.36	2.89
45	Lutein	13.691	1.13	512.43	2	2	10	1	40.46	10.40

TABLE-2
ARRANGEMENT OF COMPOUNDS IN TRAINING SET AND TEST SET

Methods	Training set compounds		Test set compounds	
	Compound No. included		Compound No. included	
Random sorting	I (50:50)	1-23	24-45	
	II (70:30)	1-32	33-45	
	III (75:25)	1-34	35-45	
	IV (25:75)	1-12	13-45	

Increasing molecular weight	I (50:50)	13, 14, 7, 11, 12, 41, 21, 2, 3, 44, 28, 20, 43, 19, 42, 6, 22, 23, 24, 26, 29, 25, 31	38, 1, 39, 40, 32, 34, 15, 16, 9, 10, 8, 30, 33, 35, 36, 37, 17, 18, 45, 4, 5, 27
	II (70:30)	13, 14, 7, 11, 12, 41, 21, 2, 3, 44, 28, 20, 43, 19, 42, 6, 22, 23, 24, 26, 29, 25, 31, 38, 1, 39, 40, 32, 34, 15, 16, 9	10, 8, 30, 33, 35, 36, 37, 17, 18, 45, 4, 5, 27
	III (75:25)	13, 14, 7, 11, 12, 41, 21, 2, 3, 44, 28, 20, 43, 19, 42, 6, 22, 23, 24, 26, 29, 25, 31, 38, 1, 39, 40, 32, 34, 15, 16, 9, 10, 8	30, 33, 35, 36, 37, 17, 18, 45, 4, 5, 27
	IV (25:75)	13, 14, 7, 11, 12, 41, 21, 2, 3, 44, 28, 20	43, 19, 42, 6, 22, 23, 24, 26, 29, 25, 31, 38, 1, 39, 40, 32, 34, 15, 16, 9, 10, 8, 30, 33, 35, 36, 37, 17, 18, 45, 4, 5, 27
Increasing HBA (naccr)	I (50:50)	45, 13, 6, 9, 10, 21, 22, 23, 24, 26, 29, 14, 25, 28, 31, 38, 7, 8, 11, 12, 19, 20, 30	32, 34, 39, 40, 41, 1, 2, 3, 33, 35, 36, 37, 42, 43, 44, 15, 16, 27, 17, 18, 4, 5
	II (70:30)	45, 13, 6, 9, 10, 21, 22, 23, 24, 26, 29, 14, 25, 28, 31, 38, 7, 8, 11, 12, 19, 20, 30, 32, 34, 39, 40, 41, 1, 2, 3, 33	35, 36, 37, 42, 43, 44, 15, 16, 27, 17, 18, 4, 5
	III (75:25)	45, 13, 6, 9, 10, 21, 22, 23, 24, 26, 29, 14, 25, 28, 31, 38, 7, 8, 11, 12, 19, 20, 30, 32, 34, 39, 40, 41, 1, 2, 3, 33, 35, 36	37, 42, 43, 44, 15, 16, 27, 17, 18, 4, 5
	IV (25:75)	45, 13, 6, 9, 10, 21, 22, 23, 24, 26, 29, 14	25, 28, 31, 38, 7, 8, 11, 12, 19, 20, 30, 32, 34, 39, 40, 41, 1, 2, 3, 33, 35, 36, 37, 42, 43, 44, 15, 16, 27, 17, 18, 4, 5
Increasing HBD (ndonr)	I (50:50)	42, 21, 22, 23, 24, 43, 1, 2, 3, 6, 8, 25, 26, 28, 29, 30, 38, 41, 44, 45, 9, 10, 13	14, 19, 20, 31, 32, 34, 7, 33, 35, 36, 39, 40, 11, 12, 27, 37, 15, 16, 17, 18, 4, 5
	II (70:30)	42, 21, 22, 23, 24, 43, 1, 2, 3, 6, 8, 25, 26, 28, 29, 30, 38, 41, 44, 45, 9, 10, 13, 14, 19, 20, 31, 32, 34, 7, 33, 35	36, 39, 40, 11, 12, 27, 37, 15, 16, 17, 18, 4, 5
	III (75:25)	42, 21, 22, 23, 24, 43, 1, 2, 3, 6, 8, 25, 26, 28, 29, 30, 38, 41, 44, 45, 9, 10, 13, 14, 19, 20, 31, 32, 34, 7, 33, 35, 36, 39	40, 11, 12, 27, 37, 15, 16, 17, 18, 4, 5
	IV (25:75)	42, 21, 22, 23, 24, 43, 1, 2, 3, 6, 8, 25	26, 28, 29, 30, 38, 41, 44, 45, 9, 10, 13, 14, 19, 20, 31, 32, 34, 7, 33, 35, 36, 39, 40, 11, 12, 27, 37, 15, 16, 17, 18, 4, 5
Increasing number of rotatable bonds (nrot)	I (50:50)	21, 7, 11, 12, 14, 20, 13, 22, 23, 24, 25, 15, 16, 17, 18, 38, 41, 2, 3, 6, 19, 26, 28	44, 29, 43, 1, 4, 31, 39, 40, 42, 5, 32, 33, 34, 35, 36, 37, 8, 9, 30, 10, 27, 45
	II (70:30)	21, 7, 11, 12, 14, 20, 13, 22, 23, 24, 25, 15, 16, 17, 18, 38, 41, 2, 3, 6, 19, 26, 28, 44, 29, 43, 1, 4, 31, 39, 40, 42	5, 32, 33, 34, 35, 36, 37, 8, 9, 30, 10, 27, 45
	III (75:25)	21, 7, 11, 12, 14, 20, 13, 22, 23, 24, 25, 15, 16, 17, 18, 38, 41, 2, 3, 6, 19, 26, 28, 44, 29, 43, 1, 4, 31, 39, 40, 42, 5, 32	33, 34, 35, 36, 37, 8, 9, 30, 10, 27, 45
	IV (25:75)	21, 7, 11, 12, 14, 20, 13, 22, 23, 24, 25, 15,	16, 17, 18, 38, 41, 2, 3, 6, 19, 26, 28, 44, 29, 43, 1, 4, 31, 39, 40, 42, 5, 32, 33, 34, 35, 36, 37, 8, 9, 30, 10, 27, 45
Increasing TPSA	I (50:50)	45, 21, 22, 23, 24, 6, 26, 13, 25, 29, 42, 9, 10, 28, 38, 8, 30, 31, 43, 41, 14, 19, 32	34, 1, 2, 3, 44, 20, 40, 11, 12, 7, 39, 33, 35, 36, 37, 27, 15, 16, 17, 18, 4, 5
	II (70:30)	45, 21, 22, 23, 24, 6, 26, 13, 25, 29, 42, 9, 10, 28, 38, 8, 30, 31, 43, 41, 14, 19, 32, 34, 1, 2, 3, 44, 20, 40, 11, 12	7, 39, 33, 35, 36, 37, 27, 15, 16, 17, 18, 4, 5
	III (75:25)	45, 21, 22, 23, 24, 6, 26, 13, 25, 29, 42, 9, 10, 28, 38, 8, 30, 31, 43, 41, 14, 19, 32, 34, 1, 2, 3, 44, 20, 40, 11, 12, 7, 39	33, 35, 36, 37, 27, 15, 16, 17, 18, 4, 5
	IV (25:75)	45, 21, 22, 23, 24, 6, 26, 13, 25, 29, 42, 9	10, 28, 38, 8, 30, 31, 43, 41, 14, 19, 32, 34, 1, 2, 3, 44, 20, 40, 11, 12, 7, 39, 33, 35, 36, 37, 27, 15, 16, 17, 18, 4, 5
Increasing log P	I (50:50)	4, 5, 17, 18, 15, 16, 11, 12, 7, 14, 41, 2, 3, 44, 13, 43, 42, 20, 28, 19, 21, 1, 40	35, 36, 37, 25, 38, 33, 39, 22, 23, 24, 6, 26, 31, 32, 34, 39, 8, 30, 9, 10, 27, 45
	II (70:30)	4, 5, 17, 18, 15, 16, 11, 12, 7, 14, 41, 2, 3, 44, 13, 43, 42, 20, 28, 19, 21, 1, 40, 35, 36, 37, 25, 38, 33, 39, 22, 23	24, 6, 26, 31, 32, 34, 39, 8, 30, 9, 10, 27, 45
	III (75:25)	4, 5, 17, 18, 15, 16, 11, 12, 7, 14, 41, 2, 3, 44, 13, 43, 42, 20, 28, 19, 21, 1, 40, 35, 36, 37, 25, 38, 33, 39, 22, 23, 24, 6	26, 31, 32, 34, 39, 8, 30, 9, 10, 27, 45
	IV (25:75)	4, 5, 17, 18, 15, 16, 11, 12, 7, 14, 41, 2	3, 44, 13, 43, 42, 20, 28, 19, 21, 1, 40, 35, 36, 37, 25, 38, 33, 39, 22, 23, 24, 6, 26, 31, 32, 34, 39, 8, 30, 9, 10, 27, 45

rotatable bonds/nrot; (6) Increasing TPSA; and (7) Increasing log P.

Formulation of QSAR models and bioactivity prediction: The activities and descriptors data were loaded in the respective fields of training set of EasyQSAR software for multiple linear regression analysis. From the regression, the QSAR equation was generated and the activities for each molecule were predicted. To keep the mean deviation of data small, log IC₅₀ value was used as criteria to predict biological activity. The model generated was then tested by substituting the test set molecular descriptor data in the respective fields. The log IC₅₀ values were predicted for the test set data.

Docking of flavonoids with PTP1B active site: PTP1B protein (PDB Id: 3A5J) was retrieved from RCSB Protein Data Bank. Heteroatoms and water molecules were removed. The protein was minimized (50:50::Steepest Descent:Conjugate Gradient) and visualized using Ramachandran plot to check any deformity. Grid box was prepared along the active site. Ligands (flavonoids class) mentioned in Table-1 were retrieved from NCBI-PubChem. The protein and ligands were prepared for docking through Autodock Vina with parameters center_x = 27.956, center_y = -13.821, center_z = -10.245, size_x = 40, size_y = 40, size_z = 40 and exhaustiveness = 8.

RESULTS AND DISCUSSION

QSAR models were developed employing multiple linear regression to calculate the predicted log IC₅₀ value for the 45 flavonoids molecules and PTP1B protein. Since all the compounds used for study were flavonoids/isoflavonoids, the basic structure was similar. It was based on methods of grouping and random sorting. Amongst all pharmacophoric features, it was observed that model generated from increasing hydrogen bond donor (ndonr) showed highest R² value of 92.45% signifying its role in flavonoid activity. This was followed by increasing molecular weight with R² value of 91.85%. The following models were developed and could be used to predict Log IC₅₀ values of the flavonoids group in the test set. The differences in experimental IC₅₀ values and predicted data were observed to be small [34-36]. Substituting the molecular descriptors in the desired equations would be beneficial to obtain log IC₅₀ values of flavonoids against PTP1B. The best fit model and equation generated for each parameter has been represented below in detail.

Random sorting: Among randomly sorting of data, model generated from 25:75 ratio gave maximum R² value (92.08%). The model equation and graph (Fig. 1) generated from QSAR analysis for prediction of log IC₅₀ is as follows:

$$\log IC_{50} = -1.148594381348E+000 + -1.882063114396E-003*(MW) + 4.339568484289E-001*(HBA) + -6.045221947662E-002*(HBD) + -2.817902080750E-003*(nrot) + 1.135939457720E-001*(naro) + -1.709118879717E-002*(TPSA) + 4.195579049184E-002*(\log P)$$

The difference between the actual and predicted values of log IC₅₀ of Training set and Test set is depicted in Table-3.

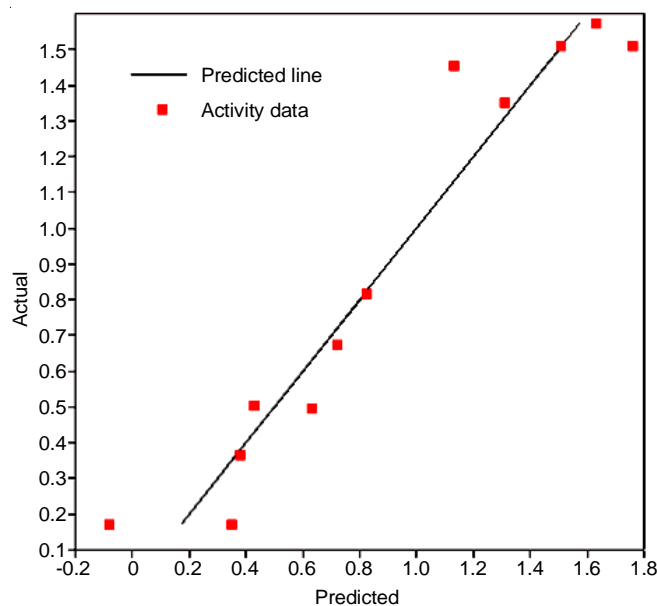


Fig. 1. QSAR plot for random sorting

Increasing molecular weight: The model generated from 25:75 ratio was observed to possess maximum R² value (91.85%). The model equation and graph (Fig. 2) generated from QSAR analysis for prediction of log IC₅₀ is as follows:

$$\log IC_{50} = -8.147055888781E+000 + 1.393057856713E-002*(MW) + 9.357902770319E-001*(HBA) + 2.045002703142E+000*(HBD) + 3.005383235447E-001*(nrot) + 5.906511654000E-001*(naro) + -1.705363036990E-001*(TPSA) + 2.040391077355E-002*(\log P)$$

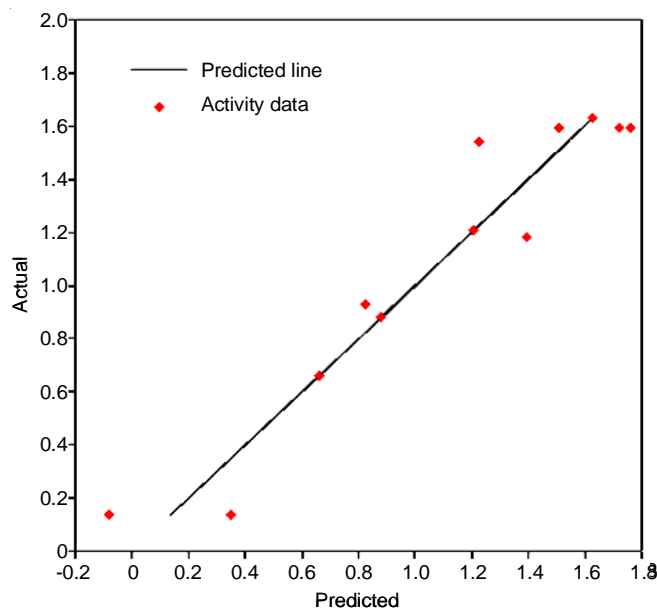


Fig. 2. QSAR plot for increasing molecular weight

The difference between the actual and predicted values of log IC₅₀ of Training set and Test set is depicted in Table-4.

Increasing hydrogen bond acceptor/HBA (naccr): The model generated from 25:75 ratio possessed maximum R² value

TABLE-3
TRAINING SET AND TEST SET VALUES

Training set				Test set							
No.	Actual log IC ₅₀	Predicted log IC ₅₀	Difference	No.	Predicted log IC ₅₀	Actual log IC ₅₀	Difference	No.	Predicted log IC ₅₀	Actual log IC ₅₀	Difference
1	1.13	1.46	0.33	13	0.01	1.206	1.196	30	0.68	0.72	0.04
2	1.76	1.51	-0.25	14	0.83	1.393	0.563	31	0.22	0.278	0.058
3	1.51	1.51	0	15	0.82	1.249	0.429	32	0.45	0.591	0.141
4	1.31	1.35	0.04	16	0.82	0.881	0.061	33	0.43	0.77	0.34
5	1.63	1.57	-0.06	17	0.81	1.389	0.579	34	0.45	0.892	0.442
6	0.38	0.37	-0.01	18	0.81	1.756	0.946	35	0.40	0.69	0.29
7	0.83	0.82	-0.01	19	0.49	1.607	1.117	36	0.40	0.913	0.513
8	0.72	0.68	-0.04	20	1.02	1.629	0.609	37	0.29	0.819	0.529
9	0.63	0.50	-0.13	21	0.67	0.88	0.21	38	0.47	1.315	0.845
10	0.43	0.50	0.07	22	0.62	0.623	0.003	39	0.71	1.356	0.646
11	0.35	0.17	-0.18	23	0.62	0.892	0.272	40	0.18	1.181	1.001
12	-0.08	0.17	0.25	24	0.62	0.806	0.186	41	1.29	1.228	-0.062
				25	0.58	0.944	0.364	42	1.48	0.837	-0.643
				26	0.37	0.863	0.493	43	1.75	1.347	-0.403
				27	1.71	0.778	-0.932	44	1.51	1.721	0.211
				28	0.49	0.662	0.172	45	-1.54	1.136	2.676
				29	0.74	0.892	0.152				

TABLE-4
TRAINING SET AND TEST SET VALUES

Training set				Test set							
No.	Actual log IC ₅₀	Predicted log IC ₅₀	Difference	No.	Predicted log IC ₅₀	Actual log IC ₅₀	Difference	No.	Predicted log IC ₅₀	Actual log IC ₅₀	Difference
1	1.21	1.21	0	13	1.90	1.347	-0.553	30	1.34	1.249	-0.091
2	1.39	1.18	-0.21	14	0.42	1.607	1.187	31	1.34	0.881	-0.459
3	0.83	0.93	0.1	15	-0.08	0.837	0.917	32	6.90	0.633	-6.267
4	0.35	0.14	-0.21	16	3.12	0.38	-2.74	33	7.21	0.431	-6.779
5	-0.08	0.14	0.22	17	2.35	0.623	-1.727	34	2.49	0.72	-1.77
6	1.23	1.54	0.31	18	2.35	0.892	-1.458	35	2.49	0.72	-1.77
7	0.88	0.88	0	19	2.35	0.806	-1.544	36	1.94	0.77	-1.17
8	1.76	1.59	-0.17	20	3.12	0.863	-2.257	37	1.92	0.69	-1.23
9	1.51	1.59	0.08	21	4.37	0.892	-3.478	38	1.92	0.913	-1.007
10	1.72	1.59	-0.13	22	2.08	0.944	-1.136	39	3.43	0.819	-2.611
11	0.66	0.66	0	23	2.14	0.278	-1.862	40	1.09	1.389	0.299
12	1.63	1.63	0	24	1.06	1.315	0.255	41	1.09	1.756	0.666
				25	3.06	1.13	-1.93	42	1.86	1.136	-0.724
				26	4.17	1.356	-2.814	43	1.47	1.311	-0.159
				27	1.87	1.181	-0.689	44	1.53	1.632	0.102
				28	2.19	0.591	-1.599	45	9.42	0.778	-8.642
				29	2.19	0.892	-1.298				

(84.19%). The model equation and graph (Fig. 3) generated from QSAR analysis for prediction of log IC₅₀ is as follows:

$$\log IC_{50} = 8.355813406245E-001 + -1.224265114555E-003*(MW) + -8.067713144688E-001*(HBA) + -2.159242933781E-001*(HBD) + -3.061861913292E-001*(nrot) + -4.493520892915E-002*(naro) + 6.322034879058E-002*(TPSA) + 3.386840954241E-001*(log P)$$

The difference between the actual and predicted values of log IC₅₀ of Training set and Test set is depicted in Table-5.

Increasing hydrogen bond donor/HBD (ndonr): The model generated from 25:75 ratio showed highest R² value (92.45%). The model equation and graph (Fig. 4) generated from QSAR analysis for prediction of log IC₅₀ is as follows:

$$\log IC_{50} = 1.475493700183E+000 + 1.212467003312E-002*(MW) + -1.938945338211E+000*(HBA) + -1.785729044976E+000*(HBD) + -1.892366013071E-001*(nrot) + -6.584223100447E-002*(naro) + 1.663790516228E-001*(TPSA) + -4.263616557878E-001*(log P)$$

The difference between the actual and predicted values of log IC₅₀ of Training set and Test set is depicted in Table-6.

Increasing number of rotatable bonds (nrot): The models generated from the parameter showed few erroneous values. 50:50 ratio showed highest R² value (53.90%). The model equation and graph (Fig. 5) generated from QSAR analysis for prediction of log IC₅₀ is as follows:

TABLE-5
TRAINING SET AND TEST SET VALUES

Training set				Test set							
No.	Actual log IC ₅₀	Predicted log IC ₅₀	Difference	No.	Predicted log IC ₅₀	Actual log IC ₅₀	Difference	No.	Predicted log IC ₅₀	Actual log IC ₅₀	Difference
1	1.14	1.14	0	13	0.69	0.944	0.254	30	-0.43	1.762	2.192
2	1.21	1.20	-0.01	14	0.35	0.662	0.312	31	-0.43	1.507	1.937
3	0.38	0.63	0.25	15	0.76	0.278	-0.482	32	0.33	0.77	0.44
4	0.63	0.65	0.02	16	1.07	1.315	0.245	33	0.08	0.69	0.61
5	0.43	0.42	-0.01	17	1.52	0.826	-0.694	34	0.08	0.913	0.833
6	0.88	0.93	0.05	18	-0.55	0.72	1.27	35	0.09	0.819	0.729
7	0.62	0.75	0.13	19	1.23	0.351	-0.879	36	-1.88	0.837	2.717
8	0.89	0.75	-0.14	20	1.23	-0.079	-1.309	37	-1.13	1.347	2.477
9	0.81	0.75	-0.06	21	0.60	1.607	1.007	38	-0.43	1.721	2.151
10	0.86	0.63	-0.23	22	1.47	1.629	0.159	39	0.55	1.249	0.699
11	0.89	0.90	0.01	23	-0.55	0.72	1.27	40	0.55	0.881	0.331
12	1.39	1.38	-0.01	24	0.20	0.591	0.391	41	0.44	0.778	0.338
				25	0.20	0.892	0.692	42	0.68	1.389	0.709
				26	0.94	1.356	0.416	43	0.68	1.756	1.076
				27	0.65	1.181	0.531	44	-1.22	1.311	2.531
				28	0.13	1.228	1.098	45	-1.7	1.632	3.332
				29	-0.61	1.13	1.74				

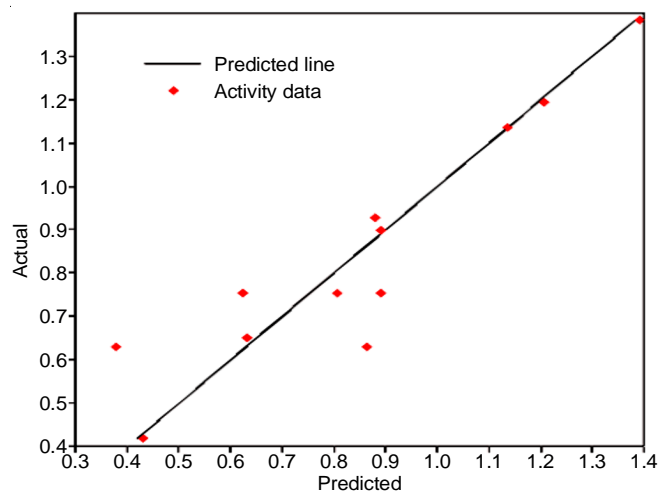


Fig. 3. QSAR plot for increasing hydrogen bond acceptor

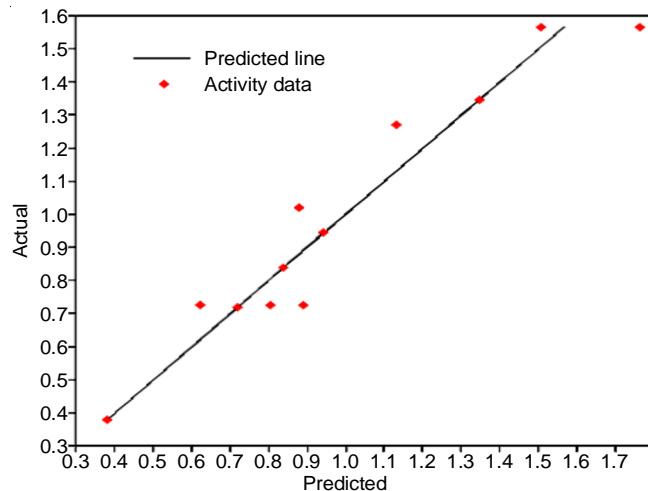


Fig. 4. QSAR plot for hydrogen bond donor

TABLE-6
TRAINING SET AND TEST SET VALUES

Training set				Test set							
No.	Actual log IC ₅₀	Predicted log IC ₅₀	Difference	No.	Predicted log IC ₅₀	Actual log IC ₅₀	Difference	No.	Predicted log IC ₅₀	Actual log IC ₅₀	Difference
1	0.84	0.84	0	13	0.38	0.863	0.483	30	2.26	0.826	-1.434
2	0.88	1.02	0.14	14	1.64	0.662	-0.978	31	0.84	0.77	-0.07
3	0.62	0.73	0.11	15	1.75	0.892	-0.858	32	1.15	0.69	-0.46
4	0.89	0.73	-0.16	16	0.72	0.72	0	33	1.15	0.913	-0.237
5	0.81	0.73	-0.08	17	1.82	1.315	-0.505	34	1.39	1.356	-0.034
6	1.35	1.35	0	18	1.82	1.228	-0.592	35	1.41	1.181	-0.229
7	1.13	1.27	0.14	19	1.56	1.721	0.161	36	0.99	0.351	-0.639
8	1.76	1.56	-0.2	20	0.58	1.136	0.556	37	0.99	-0.079	-1.069
9	1.51	1.56	0.05	21	-0.32	0.633	0.953	38	2.89	0.778	-2.112
10	0.38	0.38	0	22	-0.60	0.431	1.031	39	-0.14	0.819	0.959
11	0.72	0.72	0	23	0.58	1.206	0.626	40	2.98	1.249	-1.731
12	0.94	0.94	0	24	2.29	1.393	-0.897	41	2.98	0.881	-2.099
				25	1.45	1.607	0.157	42	2.94	1.389	-1.551
				26	2.31	1.629	-0.681	43	2.94	1.756	-1.184
				27	1.13	0.278	-0.852	44	2.96	1.311	-1.649
				28	0.88	0.591	-0.289	45	2.71	1.632	-1.078
				29	0.88	0.892	0.012				

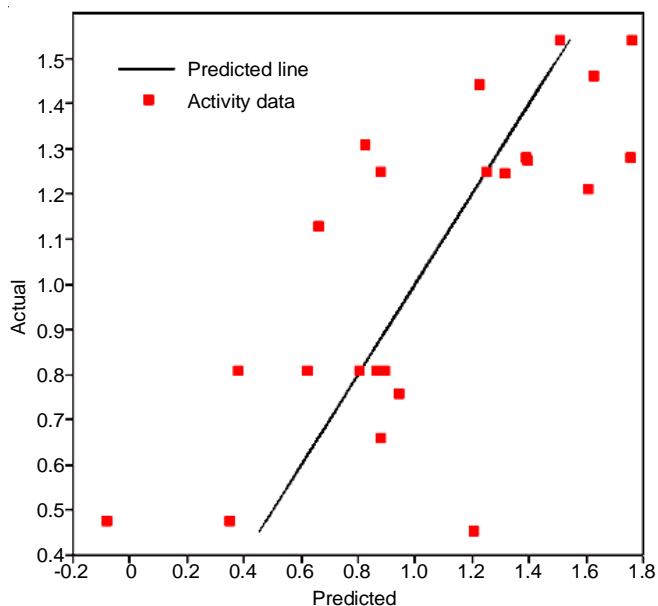


Fig. 5. QSAR plot for number of rotatable bonds

$$\log IC_{50} = -2.299946542936E-001 + -1.444328255063E-003*(MW) + -3.375857369391E-001*(HBA) + -5.832937098851E-001*(HBD) + 1.164874435960E-002*(nrot) + 2.134752195629E-002*(naro) + 5.037592655117E-002*(TPSA) + 1.414719064400E-001*(\log P)$$

The difference between the actual and predicted values of $\log IC_{50}$ of Training set and Test set is depicted in Table-7.

Increasing TPSA: The models generated from 25:75 ratio showed highest R^2 value (64.91%). The model equation and

graph (Fig. 6) generated from QSAR analysis for prediction of $\log IC_{50}$ is as follows:

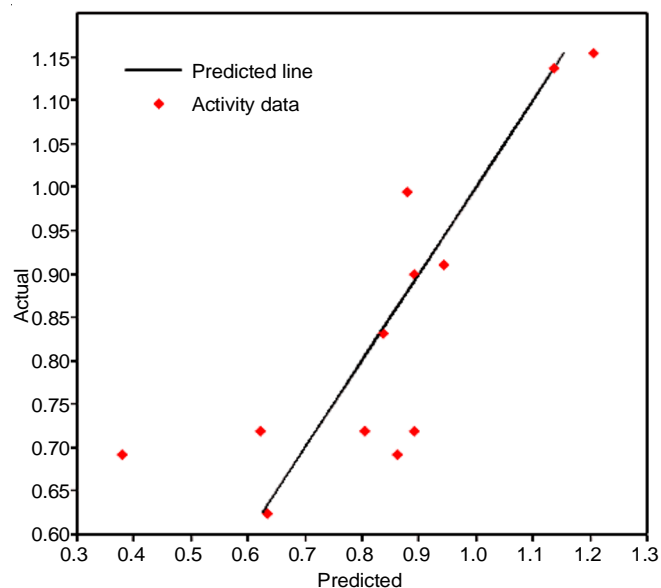


Fig. 6. QSAR plot for increasing TPSA

$$\log IC_{50} = 1.879923501054E+000 + -1.182651572300E-002*(MW) + -3.847382347768E-001*(HBA) + -7.331844373978E-001*(HBD) + -1.960444079892E-001*(nrot) + -1.685419497432E-001*(naro) + 9.834094869424E-002*(TPSA) + 5.481562673534E-001*(\log P)$$

The difference between the actual and predicted values of $\log IC_{50}$ of Training set and Test set is depicted in Table-8.

TABLE-7
TRAINING SET AND TEST SET VALUES

Training set				Test set			
No.	Actual $\log IC_{50}$	Predicted $\log IC_{50}$	Difference	No.	Predicted $\log IC_{50}$	Actual $\log IC_{50}$	Difference
1	0.88	0.66	-0.22	24	1.54	1.721	0.181
2	0.83	1.31	0.48	25	1.54	0.892	-0.648
3	0.35	0.48	0.13	26	1.61	1.347	-0.263
4	-0.08	0.48	0.56	27	1.69	1.13	-0.56
5	1.39	1.27	-0.12	28	1.43	1.311	-0.119
6	1.63	1.46	-0.17	29	1.30	0.278	-1.022
7	1.21	0.45	-0.76	30	1.65	1.356	-0.294
8	0.62	0.81	0.19	31	1.23	1.181	-0.049
9	0.89	0.81	-0.08	32	1.36	0.837	-0.523
10	0.81	0.81	0	33	1.53	1.632	0.102
11	0.94	0.76	-0.18	34	1.40	0.591	-0.809
12	1.25	1.25	0	35	1.44	0.77	-0.67
13	0.88	1.25	0.37	36	1.40	0.892	-0.508
14	1.39	1.28	-0.11	37	1.33	0.69	-0.64
15	1.76	1.28	-0.48	38	1.33	0.913	-0.417
16	1.31	1.24	-0.07	39	0.92	0.819	-0.101
17	1.23	1.44	0.21	40	1.45	0.72	-0.73
18	1.76	1.54	-0.22	41	1.35	0.633	-0.717
19	1.51	1.54	0.03	42	1.45	0.72	-0.73
20	0.38	0.81	0.43	43	1.40	0.431	-0.969
21	1.61	1.21	-0.4	44	2.93	0.778	-2.152
22	0.86	0.81	-0.05	45	0.84	1.136	0.296
23	0.66	1.13	0.47				

TABLE-8
TRAINING SET AND TEST SET VALUES

Training set				Test set							
No.	Actual log IC ₅₀	Predicted log IC ₅₀	Difference	No.	Predicted log IC ₅₀	Actual log IC ₅₀	Difference	No.	Predicted log IC ₅₀	Actual log IC ₅₀	Difference
1	1.14	1.14	0	13	0.55	0.431	-0.119	30	1.88	1.181	-0.699
2	0.88	0.99	0.11	14	1.41	0.662	-0.748	31	2.12	0.351	-1.769
3	0.62	0.72	0.1	15	1.79	1.315	-0.475	32	2.12	-0.079	-2.199
4	0.89	0.72	-0.17	16	1.17	0.72	-0.45	33	2.49	0.826	-1.664
5	0.81	0.72	-0.09	17	1.17	0.72	-0.45	34	1.86	1.356	-0.504
6	0.38	0.69	0.31	18	1.76	0.278	-1.482	35	2.29	0.77	-1.52
7	0.86	0.69	-0.17	19	0.93	1.347	0.417	36	1.88	0.69	-1.19
8	1.21	1.15	-0.06	20	1.45	1.228	-0.222	37	1.88	0.913	-0.967
9	0.94	0.91	-0.03	21	1.97	1.393	-0.577	38	1.50	0.819	-0.681
10	0.89	0.90	0.01	22	2.12	1.607	-0.513	39	1.65	0.778	-0.872
11	0.84	0.83	-0.01	23	1.77	0.591	-1.179	40	2.43	1.249	-1.181
12	0.63	0.62	-0.01	24	1.77	0.892	-0.878	41	2.43	0.881	-1.549
				25	1.18	1.13	-0.05	42	2.95	1.389	-1.561
				26	1.45	1.762	0.312	43	2.95	1.756	-1.194
				27	1.45	1.507	0.057	44	2.54	1.311	-1.229
				28	1.45	1.721	0.271	45	2.54	1.632	-0.908
				29	2.24	1.629	-0.611				

Increasing log P: The models generated from the parameter showed few erroneous results. The 75:25 ratio showed highest R² value (52.28%). The model equation and graph (Fig. 7) generated from QSAR analysis for prediction of log IC₅₀ is as follows:

$$\log IC_{50} = -3.195217933120E-001 + 1.128626176899E-003*(MW) + -3.694893472011E-001*(HBA) + -5.054256892924E-001*(HBD) + -3.294522201189E-002*(nrot) + 4.973510989186E-002*(naro) + 4.235483043750E-002*(TPSA) + 2.492750505962E-002*(\log P)$$

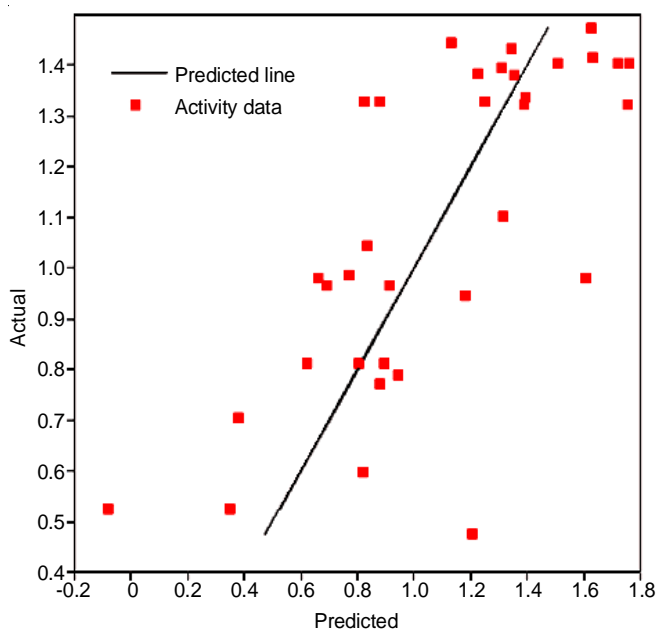


Fig. 7. QSAR plot for increasing log P

The difference between the actual and predicted values of log IC₅₀ of Training set and Test set is depicted in Table-9.

Docking of flavonoids and PTP1B active site: Table-10 shows the docking results of flavonoids with PTP1B active site and WPD loop. Fig. 8 shows the 2-dimensional docking poses of top 10 ligands. Many of the flavonoids interacts with key residues such as Tyr46, Ser216, Ala217, Arg221, Gln262. These residues play a crucial role in the protein functioning and thus have been targeted for drug development [37,38]. Previous studies have highlighted that HBD, HBA, molecular weight are molecular structure based descriptors that have been used to study inhibitors [39,40]. Comparing the docking results with the molecular descriptor properties provided in Table-1, molecular weight and HBD capability were observed to affect binding results. Vitexin (m.w. = 412.22, HBD = 7), orientin (m.w. = 428.22, HBD = 8), abyssininn II (m.w. = 348.23, HBD = 3), neorautenol (m.w. = 304.22, HBD = 1), erythraddison III (m.w. = 332.23, HBD = 2), folitenol (m.w. = 364.27, HBD = 1), erysubin E (m.w. = 380.27, HBD = 2), erysubin F (m.w. = 364.27, HBD = 2), erybreadin B (m.w. = 364.27, HBD = 1), erybreadin C (m.w. = 364.27, HBD = 2) were the top ten binding ligands.

Conclusion

Loss of PTP1B function has been observed to be effective in treating insulin resistance and enhancing insulin sensitivity. As a result, studies focus on observing the molecular properties of potent PTP1B inhibitors [41]. QSAR techniques help in finding simple equations that are beneficial to predict unknown properties of a given compound by studying the molecular structure of that compound. In this study, QSAR was conducted on some promising flavonoids that were found as potential effective PTP1B inhibitors for the treatment of T2DM. The study was conducted by using 45 flavonoid molecules each with 7 descriptors. A model was generated for each descriptor and its correlation with PTP1B inhibition was observed. They were validated for their efficiency towards test set compounds. The results have shown significant correlation with R² values

TABLE-9
TRAINING SET AND TEST SET VALUES

Training set				Test set							
No.	Actual log IC ₅₀	Predicted log IC ₅₀	Difference	No.	Actual log IC ₅₀	Predicted log IC ₅₀	Difference	No.	Predicted log IC ₅₀	Actual log IC ₅₀	Difference
1	1.31	1.39	0.08	18	1.63	1.47	-0.16	35	0.71	0.863	0.153
2	1.63	1.41	-0.22	19	0.66	0.98	0.32	36	0.97	0.278	-0.692
3	1.39	1.32	-0.07	20	1.61	0.98	-0.63	37	0.99	0.591	-0.399
4	1.76	1.32	-0.44	21	0.88	0.77	-0.11	38	0.99	0.892	-0.098
5	1.25	1.33	0.08	22	1.13	1.45	0.32	39	1.42	0.892	-0.528
6	0.88	1.33	0.45	23	1.18	0.95	-0.23	40	1.02	0.72	-0.3
7	0.35	0.53	0.18	24	0.69	0.97	0.28	41	1.02	0.72	-0.3
8	-0.08	0.53	0.61	25	0.91	0.97	0.06	42	1.01	0.633	-0.377
9	0.83	1.33	0.5	26	0.82	0.60	-0.22	43	0.98	0.431	-0.549
10	1.39	1.34	-0.05	27	0.94	0.79	-0.15	44	2.57	0.778	-1.792
11	1.23	1.39	0.16	28	1.31	1.10	-0.21	45	0.20	1.136	0.936
12	1.76	1.41	-0.35	29	0.77	0.99	0.22				
13	1.51	1.41	-0.1	30	1.36	1.38	0.02				
14	1.72	1.41	-0.31	31	0.62	0.81	0.19				
15	1.21	0.48	-0.73	32	0.89	0.81	-0.08				
16	1.35	1.43	0.08	33	0.81	0.81	0				
17	0.84	1.04	0.2	34	0.38	0.71	0.33				

TABLE-10
BINDING ENERGY (kcal/mol) OF FLAVONOIDS WITH PTP1B ACTIVE SITE

S. No.	Ligands (flavonoids/isoflavonoids)	Binding energy (kcal/mol)	RMSD (LB)	RMSD (UB)
1	Vitexin	-8.2	2.947	6.197
2	Orientin	-8.1	3.016	6.278
3	Abyssinin II	-7.8	3.937	5.155
4	Neorautenol	-7.7	26.311	28.684
5	Erythraddison III	-7.6	9.313	10.215
6	Folitenol	-7.6	9.146	13.476
7	Erysubin E	-7.5	3.332	6.552
8	Erysubin F	-7.5	14.346	16.379
9	Erybreadin B	-7.4	3.921	7.895
10	Erybreadin C	-7.4	1.126	1.839
11	Laxichalcone	-7.4	3.293	6.523
12	Erybreadin D	-7.3	5.661	8.05
13	Isovitexin	-7.3	11.829	15.808
14	Bonanniol A	-7.2	9.908	14.318
15	Epicatechin	-7.2	3.709	5.335
16	Isoorientin	-7.2	11.699	15.732
17	Macarangin	-7.2	8.651	11.898
18	Apigenin	-7.1	3.406	6.238
19	Luteolin	-7.1	3.674	5.389
20	3,5-Dihydroxy-7,3',4'-trimethoxyflavone	-7	1.957	7.788
21	Mulberofuran D	-7	2.165	5.652
22	Parvisoflavone B	-7	12.772	13.932
23	3'-O-Methyldiplacone	-6.9	10.667	13.923
24	Catechin	-6.9	3.3	5.608
25	Viscosol	-6.9	3.269	8.365
26	3,5-Dihydroxy-7-methoxy-2-(4-methoxyphenyl)-4H-chromen-4-one	-6.8	1.91	7.117
27	Erybraedin A	-6.8	2.889	4.742
28	Penduletin	-6.8	9.123	12.172
29	3'-Hydroxy-3,5,7,4'-tetramethoxyflavone	-6.7	13.763	17.376
30	(2S)-5,6,7,3',4'-Pentamethoxyflavanone	-6.5	12.781	15.114
31	2'-Methoxykuraninone	-6.5	1.977	3.394
32	Mulberofuran W	-6.2	2.493	5.542

between molecular descriptors and PTP1B inhibition. The equation generated from increasing the number of HBD was observed with maximum R² value (92.45%), followed by incre-

asing molecular weight; highlighting that both the molecular descriptors play a significant role in flavonoid activity. Docking of the ligands with the active site of PTP1B revealed that vitexin

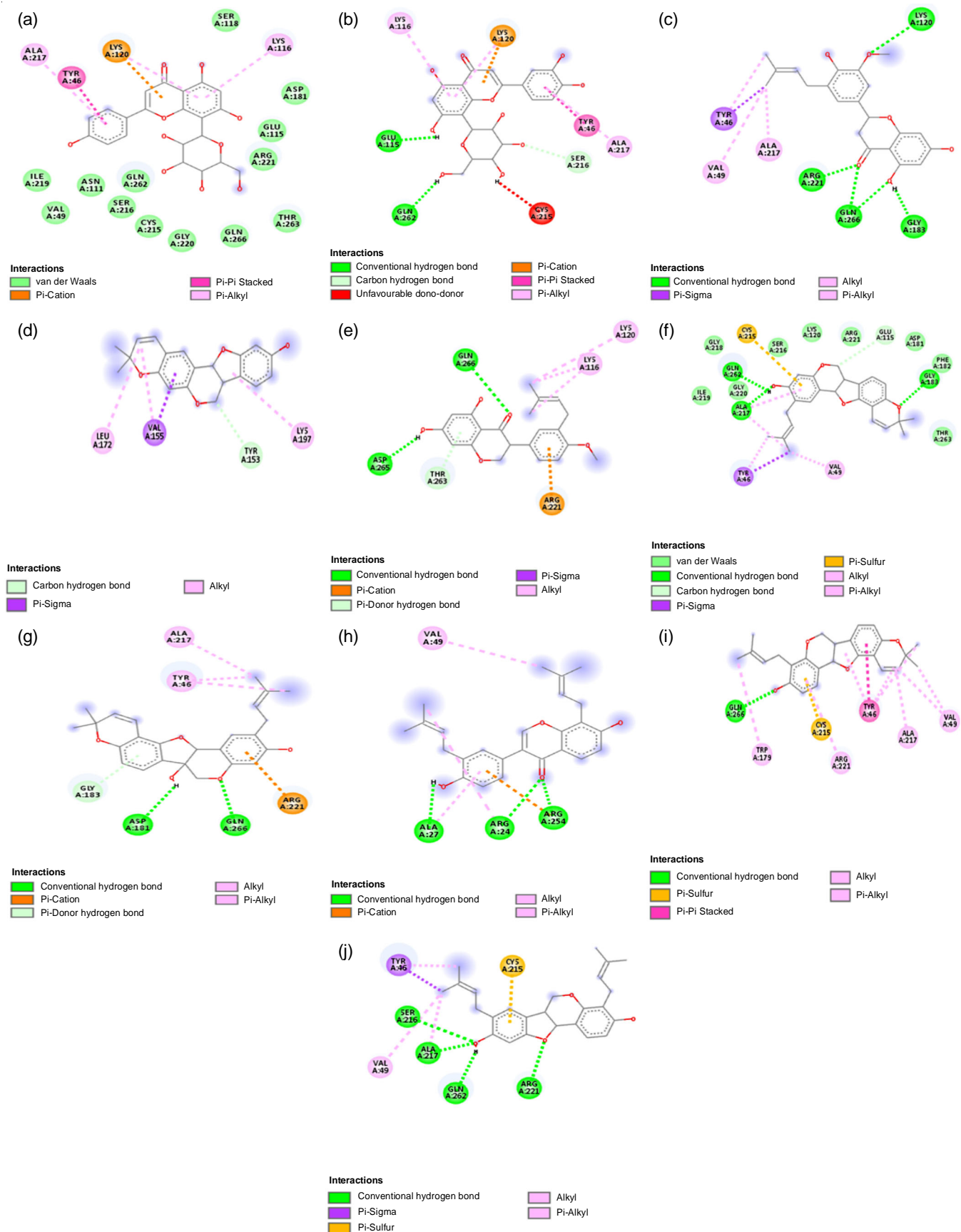


Fig. 8. Two-dimensional view of some top hit flavonoids showing interactions with amino acids of PTP1B active site and WPD loop. (a) Vitexin, (b) orientin, (c) abyssinin II, (d) neorautenol, (e) erythraddison III, (f) Folitenol, (g) erysubin E, (h) Erysubin F, (i) erybreadin B, (j) erybreadin C

with more HBD and molecular weight showed highest binding energy *i.e.* -8.2 kcal/mol. Analyzing the molecular descriptors of top ten ligands, it was observed that increasing HBD and molecular weight affected the binding energy with PTP1B. The results obtained highlighted molecular descriptors present in the flavonoids are useful for determining the inhibition of PTP1B activity. These results obtained could be helpful for designing drug candidates against PTP1B inhibition and have therapeutic implications for insulin resistance.

ACKNOWLEDGEMENTS

The authors acknowledge the Council of Scientific and Industrial Research (CSIR) India for their fellowship support.

CONFLICT OF INTEREST

The authors declare that there is no conflict of interests regarding the publication of this article.

REFERENCES

- C.F. Deacon, *Front. Endocrinol.*, **10**, 80 (2019); <https://doi.org/10.3389/fendo.2019.00080>
- V. Ormazabal, S. Nair, O. Elfeky, C. Aguayo, C. Salomon and F.A. Zuñiga, *Cardiovasc. Diabetol.*, **17**, 122 (2018); <https://doi.org/10.1186/s12933-018-0762-4>
- T.L. Laursen, C.A. Hagemann, C. Wei, K. Kazankov, K.L. Thomsen, F.K. Knop and H. Grønbaek, *World J. Hepatol.*, **11**, 138 (2019); <https://doi.org/10.4254/wjh.v11.i2.138>
- A.M. Freeman and N. Pennings, Insulin Resistance, StatPearls, Treasure Island (FL), USA, pp. 185–209 (2021).
- B.J. Neves, R.C. Braga, C.C. Melo-Filho, J.T. Moreira-Filho, E.N. Muratov and C.H. Andrade, *Front. Pharmacol.*, **9**, 1275 (2018); <https://doi.org/10.3389/fphar.2018.01275>
- M.A. Valizade Hasanloei, R. Sheikhpour, M.A. Sarram, E. Sheikhpour and H. Sharifi, *J. Comput. Aided Mol. Des.*, **32**, 375 (2018); <https://doi.org/10.1007/s10822-017-0094-6>
- J. Sun, C. Qu, Y. Wang, H. Huang, M. Zhang, H. Li, Y. Zhang, Y. Wang and W. Zou, *Mol. Biol.*, **5**, 6 (2016); <https://doi.org/10.4172/2168-9547.1000174>
- A.J. Barr, *Future Med. Chem.*, **2**, 1563 (2010); <https://doi.org/10.4155/fmc.10.241>
- R. He, Z. Yu, R. Zhang and Z. Zhang, *Acta Pharmacol. Sin.*, **35**, 1227 (2014); <https://doi.org/10.1038/aps.2014.80>
- S. Chawla, D. Gupta and A. Tiwari, *J. Pharm. Res.*, **4**, 1118 (2011).
- H. Hussain, I.R. Green, G. Abbas, S.M. Adekenov, W. Hussain and I. Ali, *Expert Opin. Ther. Pat.*, **29**, 689 (2019); <https://doi.org/10.1080/13543776.2019.1655542>
- P.M. Dewick, Medicinal Natural Products: A Biosynthetic Approach, John Wiley & Sons, Ed.: 2 (2002)
- R.A. Dixon and G.M. Pasinetti, *Plant Physiol.*, **154**, 453 (2010); <https://doi.org/10.1104/pp.110.161430>
- A.N. Panche, A.D. Diwan and S.R. Chandra, *J. Nutr. Sci.*, **5**, e47 (2016); <https://doi.org/10.1017/jns.2016.41>
- N. Koëvear, I. Glavaè and S. Kreft, *Farm. Vestn.*, **58**, 145 (2007); <https://doi.org/10.1201/NOE0824727857.ch137>
- L. Ciumarnean, M.V. Milaciu, O. Runcan, S.C. Vesa, A.L. Rachisan, V. Negrean, M.-G. Perné, V.I. Donca, T.-G. Alexescu, I. Para and G. Dogaru, *Molecules*, **25**, 4320 (2020); <https://doi.org/10.3390/molecules25184320>
- M.D. Awouafack, P. Tane and H. Morita, Isolation and Structure Characterization of Flavonoids, IntechOpen (2017); <https://doi.org/10.5772/67881>
- T. Wang, Q. Li and K. Bi, *Asian J. Pharm. Sci.*, **13**, 12 (2018); <https://doi.org/10.1016/j.ajps.2017.08.004>
- T.H. Quang, N.T.T. Ngan, C.-S. Yoon, K.-H. Cho, D.G. Kang, H.S. Lee, Y.-C. Kim and H. Oh, *Molecules*, **20**, 11173 (2015); <https://doi.org/10.3390/molecules200611173>
- E. Salinas-Arellano, A. Pérez-Vásquez, I. Rivero-Cruz, R. Torres-Colin, M. González-Andrade, M. Rangel-Grimaldo and R. Mata, *Molecules*, **25**, (2020); <https://doi.org/10.3390/molecules25153530>
- C. Proença, D. Ribeiro, M. Freitas, F. Carvalho and E. Fernandes, *Crit. Rev. Food Sci. Nutr.*, (2021); <https://doi.org/10.1080/10408398.2021.1872483>
- H.A. Jung, M.Y. Ali, H.K. Bhakta, B.-S. Min and J.S. Choi, *Arch. Pharm. Res.*, **40**, 37 (2017); <https://doi.org/10.1007/s12272-016-0852-3>
- C. Jiang, L. Liang and Y. Guo, *Acta Pharmacol. Sin.*, **33**, 1217 (2012); <https://doi.org/10.1038/aps.2012.90>
- C. Proença, M. Freitas, D. Ribeiro, J.L.C. Sousa, F. Carvalho, A.M.S. Silva, P.A. Fernandes and E. Fernandes, *Food Chem. Toxicol.*, **111**, 474 (2018); <https://doi.org/10.1016/j.fct.2017.11.039>
- M. Na, Ph.D. Thesis, Inhibitory Effect of Constituents from *Cercis chinensis* on Cellular Aging, Chungnam National University, Daejeon, Korea (2004).
- S. Li, W. Li, Y. Wang, Y. Asada and K. Koike, *Bioorg. Med. Chem. Lett.*, **20**, 5398 (2010); <https://doi.org/10.1016/j.bmcl.2010.07.110>
- F. Zargari, M. Lotfi, O. Shahraki, Z. Nikfarjam and J. Shahraki, *J. Biomol. Struct. Dyn.*, **36**, 4126 (2018); <https://doi.org/10.1080/07391102.2017.1409651>
- A.G. Dimri, R. Prasad, A. Chauhan, M.L. Aggarwal and A. Varma, *Indian J. Environ. Prot.*, **38**, 1004 (2018).
- P. Kaushik, P. Goyal, A. Chauhan and G. Chauhan, *Iran. J. Pharm. Res.*, **9**, 287 (2010).
- A. Chauhan, G. Chauhan, P.C. Gupta, P. Goyal and P. Kaushik, *Indian J. Pharmacol.*, **42**, 104 (2010); <https://doi.org/10.4103/0253-7613.64490>
- P. Kaushik, C. Abhishek and G. Pankaj, *J. Pure Appl. Microbiol.*, **3**, 169 (2009).
- P. Kaushik and A. Chauhan, *Vegetos*, **21**, 77 (2008).
- P. Kaushik and A. Chauhan, *Indian J. Microbiol.*, **48**, 348 (2008); <https://doi.org/10.1007/s12088-008-0043-0>
- P. Banjare, B. Matore, J. Singh and P.P. Roy, *Silico Pharmacol.*, **9**, 28 (2021); <https://doi.org/10.1007/s40203-021-00087-w>
- E. Arun, M. Tech. Thesis, In-silico Screening of Potential Inhibitors of Gamma-Secretase, A Key Enzyme of Alzheimer's Disease, National Institute of Technology, Rourkela, India (2013).
- R. Saikia, M.D. Choudhury, A. Das Talukdar and P. Chetia, *Asian J. Pharm. Clin. Res.*, **5**, 153 (2012).
- M.T. Ha, S. Shrestha, T.H. Tran, J.A. Kim, M.H. Woo, J.S. Choi and B.S. Min, *Arch. Pharm. Res.*, **43**, 961 (2020); <https://doi.org/10.1007/s12272-020-01269-4>
- S. Shrestha, S.H. Seong, S.G. Park, B.S. Min, H.A. Jung and J.S. Choi, *Molecules*, **24**, 2893 (2019); <https://doi.org/10.3390/molecules24162893>
- X. Zhang, H. Jiang, W. Li, J. Wang and M. Cheng, *Comput. Math. Methods Med.*, **2017**, 1 (2017); <https://doi.org/10.1155/2017/4245613>
- R.C. Wade and P.J. Goodford, *Prog. Clin. Biol. Res.*, **289**, 433 (1989).
- S.J. Patankar and P.C. Jurs, *J. Chem. Inf. Comput. Sci.*, **43**, 885 (2003); <https://doi.org/10.1021/ci020045e>